Critically Balanced Ion Temperature Gradient Turbulence in Fusion Plasmas

M. Barnes,[1,2,*] F. I. Parra,[1] and A. A. Schekochihin[1]

[1]*Rudolf Peierls Centre for Theoretical Physics, University of Oxford, Oxford OX1 3NP, United Kingdom*
[2]*Euratom/CCFE Fusion Association, Culham Science Centre, Abingdon OX14 3DB, United Kingdom*

Scaling laws for ion temperature gradient driven turbulence in magnetized toroidal plasmas are derived and compared with direct numerical simulations. Predicted dependences of turbulence fluctuation amplitudes, spatial scales, and resulting heat fluxes on temperature gradient and magnetic field line pitch are found to agree with numerical results in both the driving and inertial ranges. Evidence is provided to support the critical balance conjecture that parallel streaming and nonlinear perpendicular decorrelation times are comparable at all spatial scales, leading to a scaling relationship between parallel and perpendicular spatial scales. This indicates that even strongly magnetized plasma turbulence is intrinsically three dimensional.

Introduction.—Microscale turbulence is a ubiquitous feature of the plasmas used for magnetic confinement fusion. It is driven by kinetic instabilities feeding predominantly off a strong mean gradient in the ion temperature, and it is responsible for the majority of particle and heat transport observed in experiment. As with neutral fluid and magnetohydrodynamic turbulence, exact analytical results for kinetic plasma turbulence are rare, and numerical simulations are costly. Phenomenological scaling laws are thus useful for guiding simulation and providing gross predictions of plasma behavior in a multidimensional parameter space.

Experimental, numerical, and analytical results (cf. [1–4]) have long been used to predict the dependence of turbulent fluxes on the mean plasma gradients and on the magnetic field configuration. However, scalings based on empirical observations provide limited physical insight, and the theoretical predictions, which are predominantly based on linear or quasilinear arguments, are not sufficiently detailed to be easily falsifiable. A more detailed examination of the properties of kinetic plasma turbulence has been conducted for scales smaller than the ion Larmor radius [5–7], but it is the ion temperature gradient (ITG) driven turbulence above the Larmor scale that is most relevant for heat transport in fusion devices (cf. [8]). Recent advances in plasma fluctuation measurements [9,10] have provided turbulence spectra in this scale range; direct numerical simulations have also calculated spectra [11] and studied energy injection, transfer, and dissipation [12,13].

In this Letter, we propose a phenomenological scaling theory of ITG turbulence. A number of simple, physically motivated conjectures about the nature of this turbulence are formulated and applied to obtain fluctuation spectra from the driving scale to the ion Larmor scale. We then derive predictions for the dependence of heat flux on plasma current and ion temperature gradient. Numerical

results are presented to support our predictions and justify our conjectures.

Gyrokinetic turbulence.—Plasma fluctuations in a strong mean magnetic field are anisotropic with respect to the mean field direction and have typical frequencies that are small compared to the ion Larmor frequency, Ω_i. Such fluctuations are correctly described by the gyrokinetic approximation [14]. It assumes $\tau \Omega_i \gg 1$, $\ell_\perp/\ell_\parallel \sim \rho_i/L \ll 1$, and $\rho_i/\ell_\perp \sim 1$, where τ is the fluctuation time, ρ_i the ion Larmor radius, L the characteristic length scale of the mean dynamics, and $\ell_\parallel$ and $\ell_\perp$ are the fluctuation length scales parallel and perpendicular to the mean field, respectively. Averaging over the fast Larmor gyration eliminates gyroangle dependence. For the remaining phase space coordinates, we choose $(\mathbf{R}, E, \mu)$, where $\mathbf{R}$ is the position of the center of a particle's Larmor orbit, $E = mv^2/2$ is the kinetic energy of a particle, and $\mu = mv_\perp^2/2B$ is the magnetic moment, with m particle mass, v particle speed, $v_\perp$ its perpendicular component, and B mean magnetic field strength.

We restrict our attention to ion scale turbulence with $\rho_i/\ell_\perp < 1$, for which the guiding center position $\mathbf{R}$ and actual particle position $\mathbf{r}$ are approximately equal. The equation describing the evolution of electrostatic fluctuations in the absence of sonic flows is

$$\frac{\partial}{\partial t}\left(h_s - \frac{Z_s e \varphi}{T_s} F_{M,s}\right) + (\mathbf{v}_\parallel + \mathbf{v}_{M,s}) \cdot \nabla h_s$$
$$+ \mathbf{v}_E \cdot \nabla (F_{M,s} + h_s) = C[h_s], \qquad (1)$$

where $\delta f_s = h_s - (Z_s e \varphi/T_s)F_{M,s}$ describes the distribution of particle positions and velocities for species s, t is time, $\mathbf{v}_{M,s} = (\hat{\mathbf{b}}/\Omega_s) \times (v_\parallel^2 \hat{\mathbf{b}} \cdot \nabla \hat{\mathbf{b}} + (v_\perp^2/2)\nabla B/B)$ is the magnetic drift velocity, $\mathbf{v}_E = (c/B)\hat{\mathbf{b}} \times \nabla \varphi$ is the $\mathbf{E} \times \mathbf{B}$ drift velocity, $\hat{\mathbf{b}}$ is the unit vector along the mean field, $Z_s e$ is the species charge, e is the proton charge, T_s is the

temperature, $F_{M,s}$ is a Maxwellian distribution of velocities, and C is a Fokker-Planck collision operator.

The electrostatic potential φ is obtained by imposing quasineutrality, $\sum_s Z_s e n_s = 0$, which can be written

$$\sum_s Z_s \int d^3\mathbf{v} \left(h_s - \frac{Z_s e \varphi}{T_s} F_{M,s} \right) = 0, \qquad (2)$$

where n_s is species density. Assuming $\int d^3\mathbf{v} h_i \sim v_{\mathrm{th}}^3 h_i$, where i denotes the main ion species and v_{th} its thermal speed, Eq. (2) gives $h_i/F_{M,i} \sim Z_i e \varphi / T_i$.

Critical balance.—Because the turbulence we are considering is anisotropic, dimensional analysis alone is not sufficient to determine scalings of the fluctuation amplitudes with both $\ell_\parallel$ and $\ell_\perp$. To fix the ratio of $\ell_\parallel$ to $\ell_\perp$, we make a conjecture known as critical balance [15]: The characteristic time associated with particle streaming and wave propagation along the mean field $\ell_\parallel/v_{\mathrm{th}}$ is comparable to the nonlinear decorrelation time at each scale. This is motivated by the causality constraint: two points along the mean field can be correlated only if information can propagate between these points in the time it takes turbulence to decorrelate in the plane perpendicular to the field. It gives us a relation between parallel and perpendicular spatial scales:

$$\frac{v_{\mathrm{th}}}{\ell_\parallel} \sim \tau_{nl}^{-1} \sim \frac{v_{\mathrm{th}}}{R} \frac{\rho_i^2}{\ell_x \ell_y} \Phi_\ell, \qquad (3)$$

where τ_{nl} is the nonlinear decorrelation time, R is the major radius of the torus, $\Phi_\ell \equiv (e \varphi_\ell / T)(R/\rho_i)$, and $\varphi_\ell \equiv \varphi(\mathbf{r} + \ell) - \varphi(\mathbf{r})$. The subscripts x and y refer to the coordinates in the plane perpendicular to the mean field, with x labeling surfaces of constant magnetic flux and y labeling field lines within a constant flux surface.

Outer scale.—We define the outer scale as the scale for which the time associated with the linear drive is comparable to the nonlinear decorrelation time:

$$\tau_{nl}^{-1} \sim \omega_*^o \sim \frac{\rho_i v_{\mathrm{th}}}{\ell_y^o L_T}, \qquad (4)$$

where ω_* is the frequency associated with the ITG drive, L_T is the ITG scale length, and o labels outer scale quantities. The outer scale corresponds to the injection range, which contains the turbulence amplitude peak. We conjecture that the characteristic parallel length at the outer scale $\ell_\parallel^o$ is the parallel system size. In toroidal plasmas, this is the distance along the mean field from the outside to the inside of the torus. This distance, known as the connection length, is qR, where the safety factor q measures the pitch of the field lines. Thus,

$$\ell_\parallel^o \sim qR. \qquad (5)$$

Combining relations (3)–(5) provides a prediction for the dependence of ℓ_y^o on q and R/L_T [16]

$$\frac{\ell_y^o}{\rho_i} \sim \frac{qR}{L_T}. \qquad (6)$$

Since $qR/L_T \gg 1$ in fusion plasmas, the ratio $\rho_i/\ell_y^o \ll 1$. Thus, there is a range of scales between the outer scale and the Larmor scale, below which kinetic damping effects are expected to become significant.

The final piece of information necessary to determine scalings for the fluctuation amplitude at the outer scale, Φ_o, is a relationship between ℓ_x^o and ℓ_y^o. We conjecture that the length scales in the perpendicular plane, ℓ_x and ℓ_y, are comparable at all scales: $\ell_x \sim \ell_y \sim \ell_\perp$. Indeed, one might argue that ℓ_x is set nonlinearly at the outer scale through the shearing of radially extended eddies by zonal flow: $\ell_x^{-1} \sim \ell_y^{-1}(S_{\mathrm{ZF}}\tau_{nl})$, where S_{ZF} is the shearing rate at the outer scale due to zonal flow. For strong ITG turbulence, one expects $S_{\mathrm{ZF}}\tau_{nl} \sim 1$ [17], so that $\ell_x \sim \ell_y$ is satisfied.

Taking $\ell_x \sim \ell_y$ and using (3) and (6) in (4) gives

$$\Phi_o \sim \frac{\ell_x^o}{\rho_i} \frac{R}{L_T} \sim q \left(\frac{R}{L_T} \right)^2. \qquad (7)$$

If we assume that the ion turbulent heat flux through volume V, $Q_i \equiv V^{-1} \int d^3\mathbf{r} \int d^3\mathbf{v} (\mathbf{v}_E \cdot \nabla x)(m_i v^2/2)\delta f_i$, is dominated by the contribution from the outer scale, relations (6) and (7) imply a scaling for Q_i:

$$\frac{Q_i}{n_i T_i v_{\mathrm{th}}} \left(\frac{R}{\rho_i} \right)^2 \equiv \tilde{Q}_i \sim \frac{\rho_i}{\ell_y^o} \Phi_o^2 \sim q \left(\frac{R}{L_T} \right)^3. \qquad (8)$$

The R/L_T scaling is only valid for sufficiently large R/L_T because our simple analysis ignores the finite critical temperature gradient associated with the ITG instability.

Inertial range.—We now consider the range of scales between $\ell_\perp^o$ and ρ_i and conjecture that it is an inertial range: There is no significant dissipation or driving at scales between $\ell_\perp^o$ and ρ_i. This conjecture is to be checked *a posteriori*. To determine the spectrum in the inertial range, we identify the free energy $W = V^{-1}\sum_s \int d^3\mathbf{r} \int d^3\mathbf{v} T_s \delta f_s^2/F_{M,s}$ as a nonlinear invariant [5] and consider scale-by-scale energy balance. Because we are in an inertial range, the flux of free energy, W_ℓ/τ_{nl}, must be independent of $\ell_\perp$:

$$\frac{1}{n_i T_i} \frac{W_\ell}{\tau_{nl}} \sim \left(\frac{\rho_i}{R} \right)^2 \frac{v_{\mathrm{th}}}{R} \frac{\rho_i^2}{\ell_x \ell_y} \Phi_\ell^3 \sim \mathrm{const}. \qquad (9)$$

The dependence of Φ_ℓ on q and R/L_T is obtained by solving relation (9) for Φ_ℓ, matching to Φ_o [see (7)], using relation (6), and assuming isotropy:

$$\Phi_\ell \sim \Phi_o \left(\frac{\ell_\perp}{\ell_y^o} \right)^{2/3} \sim q^{1/3} \left(\frac{R}{L_T} \right)^{4/3} \left(\frac{\ell_\perp}{\rho_i} \right)^{2/3}. \qquad (10)$$

Parseval's theorem relates Φ_ℓ to the Fourier coefficient Φ_k, giving a scaling for the 1D fluctuation spectrum, $E(k_y)$, defined so that $\int dk_y \rho_i E(k_y) = V^{-1} \int d^3\mathbf{r} \Phi^2$:
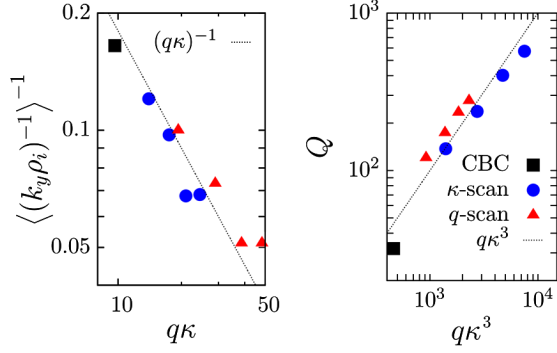
FIG. 1 (color online). (a) Expectation value of $k_y\rho_i$ versus $q\kappa$, where $\kappa \equiv R/L_T$. (b) Normalized heat flux versus $q\kappa^3$. Lines show the predicted scalings (6) and (8).

$$E(k_y) \sim k_y\rho_i|\Phi_k|^2 \sim q^{2/3}\left(\frac{R}{L_T}\right)^{8/3}(k_\perp\rho_i)^{-7/3}, \quad (11)$$

where $k_\perp = 2\pi/\ell_\perp$. Using (10) to evaluate τ_{nl}, we find $\omega_* \sim (\ell_\perp/\ell_\perp^o)^{1/3}\tau_{nl}^{-1}$, confirming that the drive is subdominant to the energy transfer in the inertial range [18].

Using relation (10) and applying critical balance (3) gives the scaling of $\ell_\parallel$ with $\ell_\perp$:

$$\frac{\ell_\parallel}{qR} \sim \left(\frac{\ell_\perp}{\rho_i}\frac{L_T}{qR}\right)^{4/3}. \quad (12)$$

Converting this into a scaling for Φ_ℓ, we obtain the parallel structure function $\Phi_\ell^2 \sim q(R/L_T)^4(\ell_\parallel/R)$.

Numerical results.—We next compare our scaling relations with numerical results obtained using the gyrokinetic code GS2 [19]. We restrict our attention to electrostatic fluctuations with perturbed electron density $\delta n_e/n_e = e(\varphi - \bar{\varphi})/T_e$, with the overline denoting a flux surface average. The magnetic geometry is as in the widely benchmarked cyclone base case (CBC) [20]: unshifted, circular magnetic-flux surface, with $r/R = 0.18$, $\hat{s} = d\ln q/d\ln r = 0.8$, and $R/L_n = 2.2$, where r is the minor radius of the flux surface, and L_n is the density gradient scale length. The parameters q and $\kappa \equiv R/L_T$ were varied over several simulations to obtain numerical scalings. These simulations employed a small amount of upwinding along the magnetic field and hyperdissipation in $k_\perp$ [21], cutting off the fluctuation spectra at $k_\perp\rho_i \simeq 1$.

In Fig. 1, we show the q and κ dependences of the normalized ion heat flux $\tilde{Q}_i$ and of

$$\frac{\ell_y^o}{\rho_i} \sim \langle(k_y\rho_i)^{-1}\rangle = \frac{\sum\limits_{k_x,k_y}(k_y\rho_i)^{-1}|\Phi(k_x,k_y)|^2}{\sum\limits_{k_x,k_y}|\Phi(k_x,k_y)|^2}, \quad (13)$$

which is a good measure of the outer scale, provided the spectrum is sufficiently steep. The simulations agree remarkably well with our predicted scalings (6) and (8) [22].
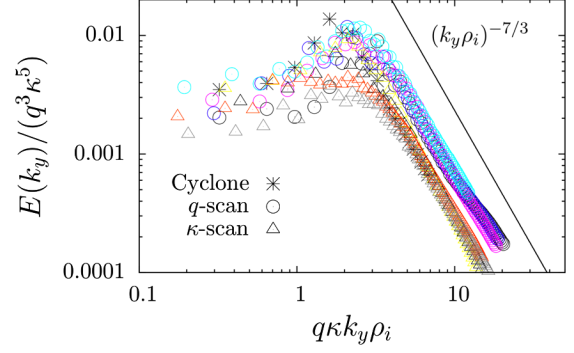

FIG. 2 (color online). Electrostatic fluctuation spectra $E(k_y)$ normalized to the predicted scaling (11) at the outer scale. We have normalized $k_y\rho_i$ using the outer scale relationship (6). Asterisks denote the cyclone base case ($q = 1.4$, $\kappa \equiv R/L_T = 6.9$); circles and triangles denote simulations where q and κ vary from 2.8 to 7.0 and 10.0 to 17.5, respectively. The solid line gives the predicted inertial range scaling (11).

The one-dimensional spectrum $E(k_y)$ is plotted vs $k_y\rho_i$ in Fig. 2 for several q and κ values. At scales smaller than the outer scale, all spectra follow the same power law, which agrees with (11).

Our predictions for the critical balance scaling (12) are tested in Figs. 3 and 4. The parallel correlation function,

$$C(k_y, \Delta\theta) \equiv \frac{\sum\limits_{k_x}\Phi(k_x, k_y, \theta = 0)\Phi^*(k_x, k_y, \theta = \Delta\theta)}{\sum\limits_{k_x}|\Phi(k_x, k_y, \theta = 0)|^2}, \quad (14)$$

is plotted in Fig. 3 for the simulation with $q = 4.2$ and $\kappa = 6.9$. Here θ is the poloidal angle of the torus so that $\Delta\theta \sim \ell_\parallel/qR$, with $\theta = 0$ at the outermost point on the flux surface. Our prediction (12) is given by the black line, which fits the data. The qR-normalized correlation length, $\overline{\Delta\theta}(k_y) \equiv \int d(\Delta\theta)C(k_y, \Delta\theta)$, is plotted in Fig. 4 for multiple q and κ values. At sufficiently large $k_y\rho_i$, the data
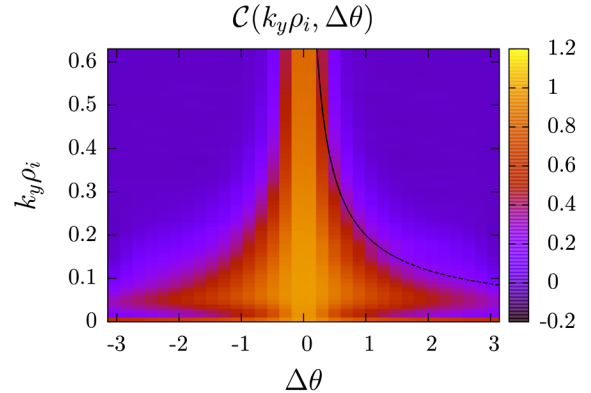

FIG. 3 (color online). Correlation function, C (14). The solid black line is $\Delta\theta \propto k_y^{-4/3}$, the critical balance scaling (12).
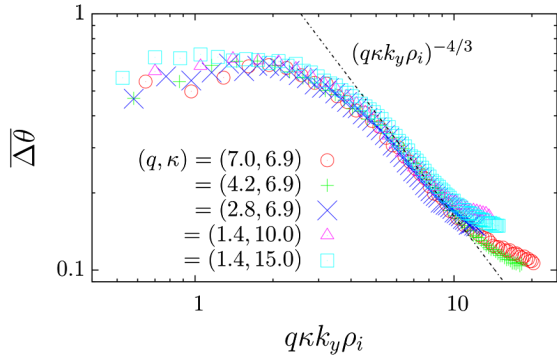
FIG. 4 (color online).   Scaling of poloidal correlation length
with $q\kappa k_y \rho_i$ for several simulations with varying q and $\kappa \equiv R/L_T$. The dashed line indicates the critical balance scaling (12).

follow the power law (12). Note that $\overline{\Delta\theta}(k_y)$ peaks at a
value of approximately unity, in agreement with (5).

Sub-Larmor scales.—Using arguments similar to
those presented above, scalings of $E(k_\perp) \sim k_\perp^{-10/3}$ and
$(k_\perp \rho_i)_c \sim \mathrm{Do}^{3/5}$ were obtained for the sub-Larmor scales
in [5] and verified numerically in [6]. Here the subscript c
denotes the cutoff wave number, and the Dorland number
$\mathrm{Do} \equiv (\tau_{\rho_i}\nu_{ii})^{-1}$ [5–7] is the kinetic plasma turbulence
analog of the Reynolds number, with τ_{ρ_i} the nonlinear
time at ρ_i and ν_{ii} the ion-ion collision frequency. Using
relations (10) and (3), we find

$$(k_\perp \rho_i)_c \sim \mathrm{Do}^{3/5} \sim q^{1/5}\left(\frac{R}{L_T}\right)^{4/5}\left(\frac{v_{\mathrm{th}}}{\nu_{ii}R}\right)^{3/5}. \quad (15)$$

Combining the results of [5] with those given here provides
a complete picture of the spectra of ITG turbulence from
the driving to dissipation scales, shown in Fig. 5.

Discussion.—The main results obtained in this Letter are
the following: a scaling of heat flux (8) and dissipation
scale (15) with q and R/L_T, a power law scaling for the
electrostatic fluctuation spectrum (11), and a relationship

between parallel and perpendicular length scales (12). The
heat flux scaling, confirmed numerically (see Fig. 1), has a
stronger dependence on R/L_T than is usually assumed by
reduced models for turbulent transport. While this has little
effect for near-marginal plasma turbulence, it may be
significant in the vicinity of steep gradient regions.

The power law prediction for the turbulence spectrum (11),
also confirmed numerically (see Fig. 2), appears to be con-
sistent with recent experimental fluctuation measurements
[10]. Along with the predictions for the dissipation scale
(15), the spectrum could be used to design large eddy simu-
lations for gyrokinetics [12] and to guide resolution choices
for direct numerical simulations. The critical balance con-
jecture (3) has proven to be robustly satisfied for the ITG
turbulence considered here (see Figs. 3 and 4). This indicates
that ITG turbulence is an inherently three-dimensional
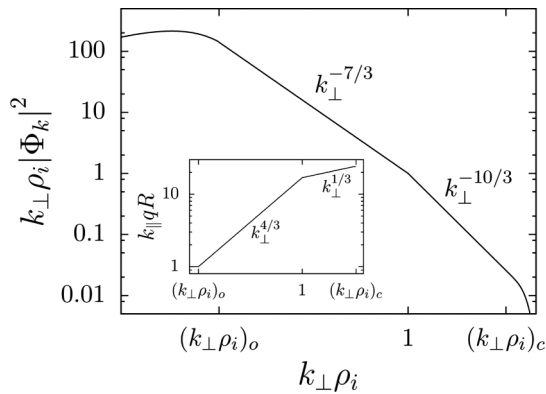phenomenon.

FIG. 5.   Cartoon of the fluctuation spectrum from the outer
scale $(k_\perp \rho_i)_o$ [Eq. (6)], to the dissipation scale $(k_\perp \rho_i)_c$
[Eq. (15)]. Scalings for $k_\perp \rho_i > 1$ are taken from [5].

*michael.barnes@physics.ox.ac.uk
[1] C. C. Petty, J. E. Kinsey, and T. C. Luce, Phys. Plasmas **11**,
     1011 (2004).
[2] M. Kotschenreuther *et al.*, Phys. Plasmas **2**, 2381
     (1995).
[3] J. E. Kinsey, R. E. Waltz, and J. Candy, Phys. Plasmas **13**,
     022305 (2006).
[4] J. W. Connor and H. R. Wilson, Plasma Phys. Controlled
     Fusion **36**, 719 (1994).
[5] A. A. Schekochihin *et al.*, Plasma Phys. Controlled Fusion
     50, 124024 (2008); A. A. Schekochihin *et al.*, Astrophys.
     J. Suppl. Ser., **182**, 310 (2009).
[6] T. Tatsuno *et al.*, Phys. Rev. Lett. **103**, 015003 (2009).
[7] G. G. Plunk *et al.*, J. Fluid Mech. **664**, 407 (2010).
[8] M. Ottaviani *et al.*, Phys. Rep. **283**, 121 (1997).
[9] A. E. White *et al.*, Phys. Plasmas **15**, 056116 (2008).
[10] P. Hennequin *et al.*, Nucl. Fusion **46**, S771 (2006).
[11] T. Görler and F. Jenko, Phys. Plasmas **15**, 102508
     (2008); A. Casati *et al.*, Phys. Rev. Lett. **102**, 165005
     (2009).
[12] A. Bañon Navarro *et al.*, Phys. Rev. Lett. **106**, 055001
     (2011).
[13] D. R. Hatch *et al.*, Phys. Rev. Lett. **106**, 115003 (2011).
[14] P. J. Catto, Plasma Phys. **20**, 719 (1978).
[15] P. Goldreich and S. Sridhar, Astrophys. J. **438**, 763 (1995);
     S. V. Nazarenko and A. A. Schekochihin, J. Fluid Mech.
     677, 134 (2011).
[16] Scaling (6) can also be obtained from linear analysis of the
     slab ITG mode, as shown in [8].
[17] S. C. Cowley *et al.*, Phys. Fluids B **3**, 2767 (1991).

[18] It is shown in [13] that there can be significant dissipation above the outer scale, but that does not affect the inertial range arguments given here.

[19] W. Dorland *et al.*, Phys. Rev. Lett. **85**, 5579 (2000).

[20] A. M. Dimits *et al.*, Phys. Plasmas **7**, 969 (2000).

[21] E. A. Belli, Ph.D. thesis, Princeton University, 2006.

[22] The heat fluxes shown in Fig. 1 are significantly larger than those reported in [20] at large κ. In order to obtain our results, it was necessary to use much larger simulation domains ($\sim 300\pi\rho_i$) than those considered in [20].